

# The Development of Forward Kinematics for a 3 Finger Adaptive Robot Gripper

Amirul S. Sadun<sup>a,\*</sup>, Jamaludin J.<sup>a</sup>

<sup>a</sup> Faculty of Engineering Technology, Universiti Tun Hussein Onn Malaysia, 84600 Batu Pahar, Johor, Malaysia

\* Corresponding author: amirul@uthm.edu.my

## ABSTRACT

This paper demonstrated the development of forwarding kinematics for a 3 Finger Adaptive Gripper by using Tracker software. The study implemented Denavit Hartenberg (DH) technique to represents the rotation matrices of a 3 link robot finger for a non-contact grasping operation. The acquired data of the joint angles ( $\theta_1, \theta_2$ , and  $\theta_3$ ) were plotted in scatter graph to find the linear relationship during the operation. Once all the related DH parameters are obtained (i.e length and linear equation), the developed forward kinematics are then validated by utilizing MATLAB simulation where the offset of the joint angles and end-effector positions/coordinates (simulation versus actual) were compared and analysed. The results show that the forward kinematics successfully represent the grasping operation of a 3 Finger Adaptive Robot Gripper. The offsets value for the joint angles and end-effector positions/coordinates were relatively small thus making the simulation results acceptable. In conjunction to the results, it is concluded that the approach of finding forward kinematics by using tracker software is feasible for a robot finger.

## INTRODUCTION

A company named ROBOTIQ introduced an underactuated robot hand called the 3-finger adaptive robot gripper as shown in Fig. 1. The robot was designed for the application in automation manufacturing and research. Moreover, the robot links were designed to have a passive compliance characteristic (elastic tendons) where it can automatically adapt to the shape of the object grasped and also simplify the control movement (Reis, Leite, & Lizarralde, 2015). Despite having a well-designed mechanism, finding the forward kinematics is challenging due to the presence of elastic tendons in the underactuated system (Licheng et al., 2016). The elastic tendon makes the forward kinematic rather complex and difficult to predict during the grasping contact (depending on the object shape and size). However, this study only focuses on estimating the forward kinematic during the non-contact operation (grasping and ungrasping).



Fig. 1 The 3-finger adaptive robot gripper.

This paper presents the development of forwarding kinematics for a 3 Finger Adaptive Robot Gripper by using Tracker software. The software is a free educational computer application that supports video playback analysis such as finding the distance, angle, and data

plotting. The study also implemented Denavit Hartenberg (DH) technique to represents the rotation matrices of a 3 link robot finger for a non-contact grasping operation. The data of the robot finger joint angles ( $\theta_1, \theta_2$ , and  $\theta_3$ ) were determined by using the video analysis and modeling tool in the Tracker software. Once all the related DH parameter is obtained, the robot hand forward kinematics were then validated by comparing the MATLAB simulation results with the actual robot hand position.

## METHODOLOGY

### Forward kinematic development approach

Tracker software supports video parameter analysis (i.e distance and angle). The user is able to define the “mass point” of the reference area at any suitable area in the video. These reference areas will automatically be detected by the software, thus enabling it to track any position changes. In this study, the detection points are located at the robot joints and end-effector as shown in Fig. 2.

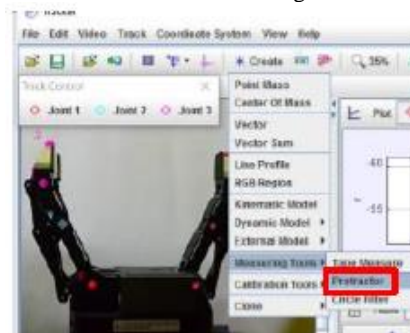
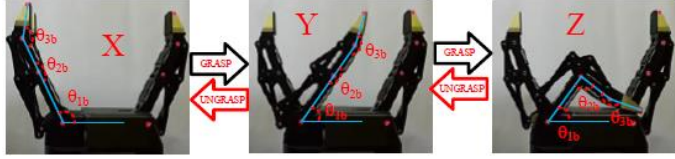


Fig. 2 Joint Angle detection by Using Tracker Software.

Each of the robot joints was patched with a bright coloured sticker (pink) for the purpose of defining the joints reference areas. It is worth noting that a for an optimum analyzing accuracy, it is best to ensure that the video is in high definition (HD) quality and completely

focused. Referring to Fig. 2, the software measuring tools (protractor) were used to track the changes of angle with respect to joint 1, joint 2 and joint 3. The data were captured for the whole video frames and can be viewed or exported from the software. The data collection was done individually for each finger (Finger A, Finger B, and Finger C) as illustrated in Fig. 3 (Finger C only). The captured data of joint angles were named  $\theta_{1b}$ ,  $\theta_{2b}$ , and  $\theta_{3b}$  respectively.



**Fig. 3** Joint Angle Data collection for Finger C (Grasping and Ungrasping).

Based on Fig. 3, it is found that a non-contact grasping or ungrasping operation consists of 3 main stages. The first stage is “X” where the robot gripper is initially resting, the next stage is “Y” where the robot gripper is in medium grasping range, and the stage “Z” is where the maximum grasping range occurred. Similar operation can be expected for all 3 finger since it is identical in term of design and mechanism. It is also expected to find a significant relationship between each of the joint angle during the grasping and ungrasping operation (Jalani, 2011). To further analyze, the joint angle data ( $\theta_{1b}$ ,  $\theta_{1b}$ , and  $\theta_{1b}$ ) were plotted as can be seen in Fig. 4. The results in Fig. 4 show the changes of joint data during the grasping (X, Y, Z order) and ungrasping (Z, Y, X order) operation. It can be observed that  $\theta_{1b}$  and  $\theta_{3b}$  are correlated whereby the joint angle increase/decrease at the same time. On the other hand, it is found that without the object contact, the  $\theta_{2b}$  is independent (no significant relation with  $\theta_{1b}$  or  $\theta_{3b}$ ). The condition is due to the fact that the elastic tendons of the underactuated mechanism only work during the contact environment.

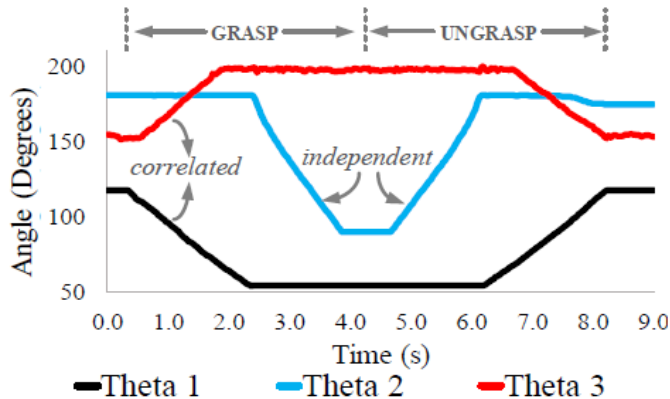


**Fig. 4** The Joint Angle Data ( $\theta_{1b}$ ,  $\theta_{1b}$ , and  $\theta_{1b}$ ).

This condition is related to the contact compliance that makes the robot gripper able to envelop the objects to be grasped and to adapt to their shape (Corrales, Jara, & Torres, 2010). However, since the study only focused on the non-contact environment, the result for  $\theta_{2b}$  is acceptable. Table 1 summarizes the data for  $\theta_{1b}$ ,  $\theta_{2b}$ , and  $\theta_{3b}$  during the grasping and ungrasping operations.

**Table 1** Data Summary

	GRASP		UNGRASP	
	X to Y	Y to Z	Z to Y	Y to X
$\theta_{1b}$	117.4° to 53.9°	Remain 53.9°	Remain 53.9°	53.9° to 117.4°
$\theta_{2b}$	Remain 180°	180° to 89.4°	89.4° to 180°	Remain 180°
$\theta_{3b}$	154° to 196.9°	Remain 196.9°	Remain 196.9°	196.9° to 154°

Furthermore, in order to calculate the forward kinematics, the data for  $\theta_{1b}$ ,  $\theta_{2b}$ , and  $\theta_{3b}$  must be computed in the form of  $\theta_1$ ,  $\theta_2$ , and  $\theta_3$ . The value for  $\theta_1$ ,  $\theta_2$ , and  $\theta_3$  can be calculated by the Eq. (1).

$$\theta_{1/2/3} = 180^\circ - \text{Captured angle of } \theta_{1b/2b/3b} \quad (1)$$

For the case of  $\theta_2$ , the independent joint angle moving range are as below (Eq. (2))

$$\theta_2 = \text{Ranged } (0^\circ \text{ until } 90.6^\circ) \quad (2)$$

Based on the data collected, finding a linear relationship between the joint angle of  $\theta_1$  and  $\theta_3$  is possible since both data are correlated. The approach was similar to (Jalani, 2011), whereby the data of  $\theta_1$  versus  $\theta_3$  were plotted on a scatter graph in order to find the linear equation. The results are as shown in Fig. 5.

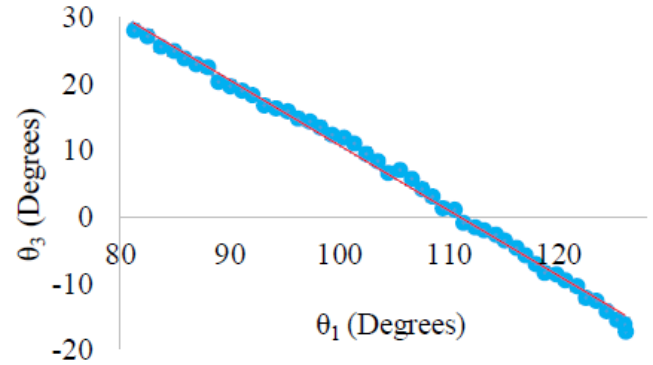


**Fig. 5** Finding a linear Relationship Between  $\theta_1$  and  $\theta_3$  (Red line).

The linear relationship between  $\theta_1$  and  $\theta_3$  for each robot finger can be written as Eq. (3).

$$\theta_3 = -0.98240 \theta_1 + 109.02 \quad (3)$$

For the purpose of this study, the Eq. (2) and Eq. (3) were converted in a form of radians to suit the programming platform in MATLAB. Thus, the equations become Eq. (4) and Eq. (5),

$$\theta_2 = \text{Range } (0 \text{ until } 1.581) \quad (4)$$

$$\theta_3 = -0.98240 \theta_1 + 1.902 \quad (5)$$

The related length parameters were measured as shown in Fig. 6 and the data are summarized in Table 2.

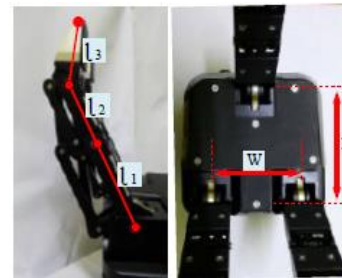


**Fig. 6** Parameter Measurement

**Table 2** Parameter Measurement Data.

$l_1$ (cm)	$l_2$ (cm)	$l_3$ (cm)	W (cm)	L (cm)
5.7	3.8	3.5	7.7	10

### Denavit Hartenberg representation

The findings from Eq. (4) and Eq. (5) can be computed by using Denavit Hartenberg technique (Craig, 2004). Since all 3 fingers are similar, this section will be outlining the method of finding the DH representation for only 1 finger. Table 3 shows the general DH parameter for 3 link robot finger.

**Table 3** Denavit Hartenberg Parameter for a 3 Link Robot Finger.

$i$	Twist Angle, $\alpha_i$ (rad)	Link Length, $a_i$ (cm)	Link Offset, $d_i$ (cm)	Joint Angle, $\theta_i$ (rad)
1	$0.78 + \alpha_1$	5.7	0	$\theta_1$
2	0	3.8	0	$\theta_2$
3	0	3.5	0	$-0.9824 \theta_1 + 1.902$

The general transformation formula is as Eq. (6).

$$A_i = \begin{bmatrix} \cos \theta_i & -\sin \theta_i \cos \alpha_i & \sin \theta_i \sin \alpha_i & a_i \cos \theta_i \\ \sin \theta_i & \cos \theta_i \cos \alpha_i & -\cos \theta_i \sin \alpha_i & a_i \sin \theta_i \\ 0 & \sin \alpha_i & \cos \alpha_i & d_i \\ 0 & 0 & 0 & 1 \end{bmatrix} \quad (6)$$

By substituting the parameters in Table 1 in (6), each link transformation can be represented as Eq. (7), Eq. (8), and Eq. (9).

Link 1,  $A_1$

$$= \begin{bmatrix} \cos \theta_1 & -\sin \theta_1 \cos(0.78 + \alpha_1) & \sin \theta_1 \sin(0.78 + \alpha_1) & a_1 \cos \theta_1 \\ \sin \theta_1 & \cos \theta_1 \cos \alpha_1 & -\cos \theta_1 \sin(0.78 + \alpha_1) & a_1 \sin \theta_1 \\ 0 & \sin \alpha_1 & \cos \alpha_1 & d_1 \\ 0 & 0 & 0 & 1 \end{bmatrix} \quad (7)$$

Link 2,  $A_2$

$$= \begin{bmatrix} \cos \theta_2 & -\sin \theta_2 & 0 & a_2 \cos \theta_2 \\ \sin \theta_2 & \cos \theta_2 & 0 & a_2 \sin \theta_2 \\ 0 & 0 & 1 & d_2 \\ 0 & 0 & 0 & 1 \end{bmatrix} \quad (8)$$

Link 3,  $A_3$

$$= \begin{bmatrix} \cos(-0.9824 \theta_1 + 109.02) & -\sin(-0.9824 \theta_1 + 109.02) & 0 & a_3 \cos(-0.9824 \theta_1 + 109.02) \\ \sin(-0.9824 \theta_1 + 109.02) & \cos(-0.9824 \theta_1 + 109.02) & 0 & a_3 \sin(-0.9824 \theta_1 + 109.02) \\ 0 & 0 & 1 & d_3 \\ 0 & 0 & 0 & 1 \end{bmatrix} \quad (9)$$

Finally, the full forward kinematics transformation is as Eq. (10).

$$T_3 = A_1 \times A_2 \times A_3 \quad (10)$$

### Validation of kinematics

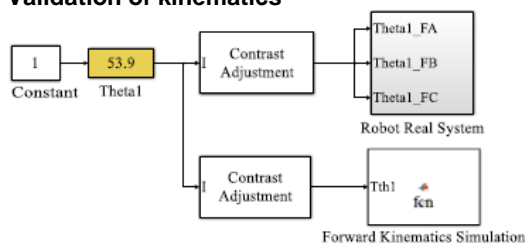


Fig. 7 MATLAB Simulink Blocks for Validation Stage

Based on Fig. 7, the “Robot Real System” block utilized a Modbus RTU protocol, which was specifically programmed to control the joint angle of the robot gripper (similarly used in (Sadun, Jalani, & Jamil, 2014)). On the other hand, the “Forward Kinematics Simulation” block utilized the MATLAB function to create a simulation (animation) of an actual robot gripper in 3D coordinate plotting. The test was done by setting up the  $\theta_1$  value for the simulation and actual robot gripper. Once the actual robot gripper moved to the specified position, the coordinate of the end-effector was obtained by manual measurement while the coordinate for end-effector in the simulation was obtained from the 3D coordinate plotting. Note that the contrast adjustment blocks are used to convert the degrees into radians data format.

## RESULTS AND DISCUSSION

### Initial resting position

Figure 8 shows the initial resting position. Referring to Table 4, the results show minor offset for the simulation data in comparison with the actual joint angle data. The simulation results in  $\theta_1$  yield an offset value of  $4.3^\circ$  while  $\theta_3$  offset value is  $2.5^\circ$ . These offsets are relatively small compared to the angular range of  $\theta_1$  and  $\theta_3$ . Thus, the offsets are considered acceptable while expecting a minor offset on the full range of the simulation.

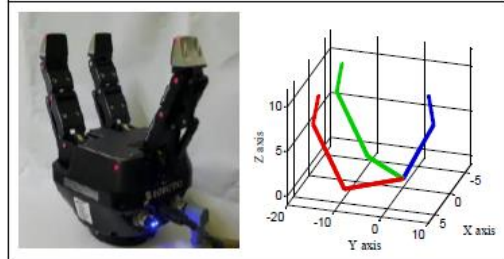


Fig. 8 Initial Resting Position

Table 4 Joint Angle Data for Initial Resting Position.

Joint Angle	Simulation	Actual	Offset
$\theta_1$	$113.1^\circ$	$117.4^\circ$	$4.3^\circ$
$\theta_2$	$180^\circ$	$180^\circ$	$0^\circ$
$\theta_3$	$151.5^\circ$	$154^\circ$	$2.5^\circ$

Table 5 Coordinate Data for Finger A.

Coordinate (cm)	Finger A		
	Simulation	Actual	Offset
X	-0.0116	0	0.0116
Y	3.482	3.7	0.218
Z	11.75	11.7	0.05

Table 6 Coordinate Data for Finger B.

Coordinate (cm)	Finger B		
	Simulation	Actual	Offset
X	-3.85	-3.85	0
Y	-13.22	-13.5	0.28
Z	11.72	11.7	0.02

Based on the forward kinematics results in Table 5, Table 6 and Table 7, all 3 robot fingers indicate similar forward kinematic results (as expected). The end-effector coordinates data shows that the offset for the resting position are small (less than 1 cm) which demonstrate the accuracy of the forward kinematics simulation.

### Medium grasping position

Fig. 9 illustrates the forward kinematics validation results for the medium grasping position while the data for joint angle and coordinates data are summarized in Table 10, Table 11, Table 12 and Table 13.

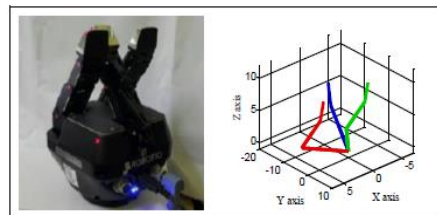


Fig. 9 Medium Grasping Position

Table 8 Joint Angle Data for Medium Grasping Position.



Joint Angle	Simulation	Actual	Offset
$\theta_1$	60.8°	53.9°	6.9°
$\theta_2$	180°	180°	0°
$\theta_3$	198.8°	196.9°	1.9°

Table 8 to reveals that there is a slight increase in the offset value for the results show that the offset value for  $\theta_1$  (6.9°) at the medium grasping position. However, the simulation results for  $\theta_3$  yield an offset value of 1.9° which a decrement from the result in initial resting position. Nevertheless, these offsets are still acceptable since they are relatively small compared to the full angular range of  $\theta_1$  and  $\theta_3$ .

The forward kinematics results for medium grasping position in Table 9, Table 10 and Table 11 show that the simulation coordinates for the end-effector are still acceptable in comparison with the actual end-effector position. However, the offset for Z axis increase dramatically from 0.02 (initial resting) to 0.57 (medium grasping) possibly as a result of a larger offset of  $\theta_1$  value in the forward kinematics simulation.

**Table 9** Coordinate Data for Finger A.

Coordinate (cm)	Finger A		
	Simulation	Actual	Offset
X	-0.0082	0	0.0082
Y	-8.464	-8	0.464
Z	10.93	11.5	0.57

**Table 10** Coordinate Data for Finger B.

Coordinate (cm)	Finger B		
	Simulation	Actual	Offset
X	-3.85	-3.85	0
Y	-1.1133	-1.5	0.386
Z	10.93	11.5	0.57

**Table 11** Coordinate Data for Finger C.

Coordinate (cm)	Finger C		
	Simulation	Actual	Offset
X	3.85	3.85	0
Y	-1.133	-1.5	0.367
Z	10.93	11.5	0.57

### Maximum grasping position

Fig. 10 illustrates the forward kinematics validation results for the maximum grasping position while the data for joint angle and coordinates data are summarized in Table 12, Table 13, Table 14 and Table 15.

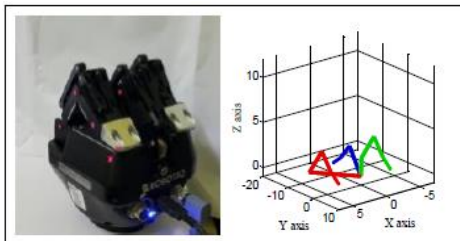


**Fig. 10** Maximum Grasping Position

**Table 12** Joint Angle Data for Maximum Grasping Position.

Joint Angle	Simulation	Actual	Offset
$\theta_1$	58.3°	53.9°	4.4°
$\theta_2$	85.2°	89.4°	4.2°
$\theta_3$	199.2°	196.9°	2.3°

Referring to Table 12, the results show that the offset value for  $\theta_1$ ,  $\theta_2$  and  $\theta_3$  are 4.4°, 4.2° and 2.3° respectively. These results are acceptable and are still considered as a minor offset compared to the full angular range for all 3 joints.

**Table 13** Coordinate Data for Finger A.

Coordinate (cm)	Finger A		
	Simulation	Actual	Offset
X	-0.0123	0	0.0123
Y	-11.03	-10.5	0.53
Z	0.1216	0.5	0.378

**Table 14** Coordinate Data for Finger B.

Coordinate (cm)	Finger B		
	Simulation	Actual	Offset
X	-3.85	-3.8	0.05
Y	1.563	1.5	0.063
Z	0.068	0.5	0.431

**Table 15** Coordinate Data for Finger C.

Coordinate (cm)	Finger C		
	Simulation	Actual	Offset
X	3.85	3.8	0.05
Y	1.563	1.5	0.063
Z	0.068	0.5	0.431

Finally, referring to Table 13, Table 14 and Table 15, the forward kinematics simulation results for the maximum grasping position were accurately represented. Despite having a minor offset on the joint angle and coordinate data, the results are still considered acceptable (less than 1cm offset).

### CONCLUSION

This paper demonstrated the development of forwarding kinematics for a 3 Finger Adaptive Robot Gripper by using Tracker software. The software is proven to be reliable in analyzing the pre-recorded video with the available video analysis tool (protractor measurement). The data recorded were analyzed, and the linear relationship between  $\theta_1$  and  $\theta_3$  were obtained. Implementing Denavit Hartenberg (DH) technique validates the results showing that the simulation of the forward kinematics successfully represents the robot gripper. The offset value for the simulation and the actual joint angle were relatively small for initial resting, medium and maximum grasping position (less than 7°). The results were considered acceptable since it is relatively small compared to the full angular range of  $\theta_1$ ,  $\theta_2$ , and  $\theta_3$ . Moreover, further validation showed that the simulation of the forward kinematics accurately represents the robot gripper end-effectors coordinate values. The offset between simulation and actual robot gripper end-effector coordinate were also considered small and acceptable (less than 1 cm). Based on the validation results, it can be concluded that the development of forwarding kinematics for a 3 Finger Adaptive Robot Gripper by using Tracker software was a success. For a non-contact environment, the results show that the Tracker video analysis offers a solid video analysis tools that can be used in future studies (i.e analyzing the joint angles during contact environment or grasping with objects).

### ACKNOWLEDGEMENT

This work was financially supported by the Fundamental Research Grant Scheme (FRGS), Vote 1480. The authors also wish to thank the Faculty of Engineering Technology, Universiti Tun Hussein Onn Malaysia for providing a platform to carry out the research activities.

### REFERENCES

- Corrales, J. A., Jara, C. A. Torres, F. 2010. Modelling and simulation of a multi-fingered robotic hand for grasping tasks. *11th International Conference on Control Automation Robotics & Vision*, 1577–1582.
- Jalani, J.. 2011. Development Of The Forward Kinematics For Robot Fingers By Using Roborealm. Arpapress.Com, 7, 172–180.
- Craig, J.J. 2004. Introduction to Robotics: Mechanics and Control. 3<sup>rd</sup> Edition, 1-400.
- Reis, M.F., Leite, A.C., Lizzaralde, F. 2015. Modeling and Control of a Multifingered Robot Hand for Object Grasping and Manipulation Tasks. *54th IEEE Conference on Decision and Control (CDC)*, 159-164.